

NONLINEAR INTERACTIONS BETWEEN WATER WAVES AND CURRENTS

Roger Matsumoto Moreira

School of Engineering, Fluminense Federal University
R. Passos da Pátria 156, bl.D, sl.505, Niterói, R.J., Brazil.
CEP: 24210-240. E-mail: rmmoreira@engenharia.uff.br

Abstract. *The interaction between a train of linear water waves with gentle steepness over “rapidly” and “slowly” varying currents is studied. The nonlinear numerical results show that surface waves can be focused by adverse surface currents, leading to very rough water surfaces, with sometimes a partial reflection being observed. Upstream of these regions the surface of the water is especially smooth as all short waves are eliminated. A good agreement between the fully nonlinear results and linear ray theory was found for “slowly” varying currents. In this case, accurate linear solutions are obtained when very small initial wave steepnesses are considered. For sharp current gradients, wave blocking and breaking are more prominent. Reflection was also observed at the blocking region when sufficiently strong adverse currents are imposed, confirming that at least part of the wave energy that builds up within the caustic can be released in the form of wave breaking and partial reflection.*

Keywords. *Wave-current interactions, nonlinear effects, ray theory, boundary integral method.*

1. Introduction

Wave-current interactions occur in nature over a wide range of hydrodynamic length scales. Giant waves have been registered in some parts of the world, especially off the east coast of South Africa, where long waves are focused by the Agulhas current. Short surface waves propagating into a strong enough opposing current can be blocked, such as at the entrances of tidal inlets. In both cases the adverse current augments the wave height and steepness, resulting in increased breaking and thus adding to the hazards of navigation.

The effects of underlying currents on water waves have been known for centuries by navigators and are of special interest for physicists and coastal engineers. The change in wave pattern due to an ocean current is often recognisable in aerial photos and satellite pictures. A better understanding of the resultant water surface can, for example, help to interpret data from radar images of the ocean surface. Thus the study of wave-current interactions has been a topic of active research among scientists for many years with several experimental and theoretical approaches. The varied physical aspects in which these interactions occur and the different mathematical approaches that are applicable to them can be found in the review papers of Peregrine (1976), Jonsson (1990) and Thomas & Klopman (1997).

A particular area of interest is the interaction between short-scale gravity waves and strong large-scale currents. In this case the time and length scales over which the current varies is much larger than the wave period or wavelength. If these waves propagate into a strong enough opposing current, then their group velocity could reduce to zero causing the waves to be blocked. A region almost free of wave activity is formed upstream from the blocking point while a strong increase in wave steepness is observed downstream from this point, leading to breaking waves. This represents an important phenomenon in areas where sea waves interact with strong ebb currents or a river outflow. Large current gradients are likely to occur due to the jet-like structure of these flows.

Short surface waves propagating over a steady but non-uniform current tend to undergo refractive changes in length, direction and amplitude. The changes in length and direction depend on kinematical considerations only. Under certain conditions a simple linear ray theory can predict these properties accurately. However, changes in the wave amplitude are less straightforward. Nonlinear interactions between the waves and the components of the current may affect the amplitude of the surface waves. Indeed several theoretical papers have been published aiming to clarify the wave transformation that occurs when the wave intensity is sufficient for nonlinear effects to begin to be important. For waves propagating against adverse currents, solutions based on linear ray theory associated with wave breaking and reflection were found near the blocking point using different mathematical approaches (see e.g. Peregrine & Thomas 1979 and Peregrine & Smith 1979).

The complexity of the wave field and the theoretical difficulties to understand the dynamics nearby the blocking point stimulated several researchers to carry on experimental works in this field. Recent laboratory measurements of the wave envelope considering very gentle monochromatic waves propagating through the blocking region (Chawla 1999, Chawla & Kirby 2002) showed that complete reflection of small wave amplitudes can occur, confirming linear and near-linear theory predictions. Furthermore, for increasing wave amplitudes, a transition region between waves being completely reflected with no breaking to completely breaking with no reflection was observed. Partial wave blocking was also reported.

Modelling the wave transformation that occurs in the blocking region is a difficult task. The sharp steepening of waves downstream the blocking point induced by large surface current gradients makes the linear approach inappropriate. In addition, solutions involving both incident and reflected waves have to be considered in order to fully understand caustic problems. An amplitude evolution model based on the conservation of wave action, including viscous dissipation and wave breaking, was proposed by Suastika *et al.* (2000). Their model overestimates wave transmission through the blocking point and discrepancies between experimental and numerical results were found in the blocking region.

To shed further light on the subject, we investigate through numerical simulations the behaviour of a train of linear water waves interacting with “rapidly” and “slowly” varying surface currents. In our simplified model the fully nonlinear, unsteady, boundary-integral method developed by Dold & Peregrine (1986) is modified in order to include the underlying current. The current is assumed to be two-dimensional and stationary, being induced by a distribution of singularities located beneath the free surface (Moreira & Peregrine 2001, Moreira 2001).

2. Boundary value problem

The fluid flow is assumed to be inviscid and incompressible. The singularities - a pair of fixed counter-rotating vortices or a system of sinks/sources - are distributed below the free surface and are defined in terms of their position and strength according to the required underlying flow. It is assumed that the flow is irrotational outside the singular cores and away from the free surface. The irrotational velocity field $\vec{u}(x,y,t)$ is then given by the gradient of a full velocity potential $\Phi(x,y,t)$ which satisfies Laplace's equation in the fluid domain, excluding the singular points,

$$\nabla^2 \Phi = 0 . \quad (1)$$

From Green's theorem all the interior properties of the fluid can be determined by its properties at the boundaries alone. The entire motion can then be modelled by considering a point discretisation of the surface. The velocity of the fluid at the surface is determined using,

$$\vec{u} = \nabla \Phi = \frac{\partial \Phi}{\partial n_1} \vec{n}_1 + \frac{\partial \Phi}{\partial n_2} \vec{n}_2 , \quad (2)$$

where \vec{n}_1 and \vec{n}_2 are the tangential and normal unit vectors respectively.

The introduction of the singular points in our model is done by decomposing our full velocity potential Φ into a regular part ϕ_w (due to surface waves) and a singular part ϕ_s (due to the singularities),

$$\Phi = \phi_w + \phi_s , \quad (3)$$

which satisfies Laplace's equation. The kinematic boundary condition to be satisfied at the free surface is based on a continuum idea that a fluid particle described by a position vector $\vec{r}(x,y,t)$ on the moving free surface remains on it. Therefore,

$$\frac{D \vec{r}}{Dt} = \nabla \Phi . \quad (4)$$

The dynamic surface condition is given by Bernoulli's equation,

$$\frac{D \Phi}{Dt} = \frac{1}{2} |\nabla \Phi|^2 - \frac{p}{\rho} - gy . \quad (5)$$

Here y is the elevation of the free surface above the undisturbed water level, g is the acceleration due to gravity (acting vertically downwards), ρ is the fluid density and p is the pressure on the exterior side of the surface. The pressure p can be chosen to approximate the effects of wind or a localised pressure on the surface, though it is not used in the calculations.

We assume that the water is deep, satisfying the condition $|\nabla \Phi| \rightarrow 0$ as $y \rightarrow -\infty$. For convenience a periodic domain is used. Then the velocity potential $\Phi(x,y,t)$ and the velocity $\vec{u}(x,y,t)$ are required to be continuous at the vertical boundaries such that,

$$\nabla \Phi(0,y,t) = \nabla \Phi(2\pi,y,t), \quad (6)$$

for $-\infty < y \leq 0$ and $t > 0$. Here the length units are chosen to make the period equal to 2π . To complete the model an initial condition for the free surface is required and given by,

$$\eta(x) = \eta_0(x), \quad \Phi(x, \eta) = \Phi_0(x, \eta_0), \quad (7)$$

for $t = 0$. Attention is directed to cases of surface waves with initially uniform wavenumber with gentle steepness.

3. Fully nonlinear boundary-integral solver

The boundary value problem is solved using an adapted version of the fully nonlinear potential flow program developed by Dold & Peregrine (1986). The method consists of applying a boundary-integral method to a free surface flow problem, which reduces significantly the computational demand for the calculation of the fluid motion since only surface properties are evaluated. The solution method is based on solving an integral equation that arises from Cauchy's integral theorem for functions of a complex variable. The original numerical scheme is modified for the inclusion of singularities.

3.1. Integral formulation

The calculation of the free surface velocity $\nabla\phi_w$ becomes relatively simple when applying Cauchy's integral theorem. If we take $z = x + iy$ as the complex equivalent of the position vector $\vec{r} = (x, y)$ for a certain time t , ϕ_w is an analytic function of z . The wave complex potential gradient is defined as,

$$q_w = \frac{\partial\phi_w}{\partial x} - i \frac{\partial\phi_w}{\partial y}, \quad (8)$$

which is also an analytic function of z . On the boundary, z is treated as a function of the parameter ξ and time t . Similarly, taking $Z(\xi, t)$ as the complex equivalent of the surface profile vector $\vec{R} = (x(\xi, t), y(\xi, t))$, q_w can be defined in terms of the tangential and normal gradients of ϕ_w at the surface,

$$\bar{q}_w = \frac{\partial Z}{\partial n_1} \left(\frac{\partial\phi_w}{\partial n_1} + i \frac{\partial\phi_w}{\partial n_2} \right) \quad (9)$$

We assume that the surface contour C that surrounds the fluid domain is smooth, then applying Cauchy's integral theorem leads to,

$$\frac{\partial\phi_w}{\partial n_2} = \frac{1}{\pi} \oint_C \Im \left(\frac{\partial Z / \partial n_1}{Z - Z'} \right) \frac{\partial\phi_w'}{\partial n_2} dn_1 + \frac{1}{\pi} \oint_C \Re \left(\frac{\partial Z / \partial n_1}{Z - Z'} \right) \frac{\partial\phi_w'}{\partial n_1} dn_1, \quad (10)$$

in which $\partial\phi_w / \partial n_2$ can be determined since $\partial\phi_w / \partial n_1$ can be calculated directly. The arclength n_1 is a scalar variable which increases in an anticlockwise sense around the closed contour C . The primed variables Z' , $\partial\phi_w' / \partial n_1$ and $\partial\phi_w' / \partial n_2$ are evaluated at points on the surface corresponding to n_1' .

3.2. Periodicity and conformal mapping

For the purpose of evaluating $\partial\phi_w / \partial n_2$ when the surface is periodic in x , the “infinite” fluid surface is transformed into a finite closed contour via a conformal mapping of the form,

$$\zeta(\xi, t) = e^{-iZ(\xi, t)}. \quad (11)$$

No generality is lost in assuming time and space dimensions to be suitably scaled by choosing a certain length L to make this period exactly 2π . Figure (1) shows schematically the z and ζ -planes with their undisturbed free surface F and a pair of singularities S_1 and S_2 with their corresponding images reflected onto the free surface, which is the appropriate choice for deep water. In this approach any singularities outside the fluid domain may be included in ϕ_s .

3.3. Free surface currents

To model the required underlying flow, a pair of vortices and a distribution of sinks and sources are selected aiming to represent “rapidly” and “slowly” varying surface currents in a periodic domain. In order to apply Cauchy's integral theorem, a conformal mapping of the form defined in expression (11) is applied to the singular potential velocity ϕ_s . For

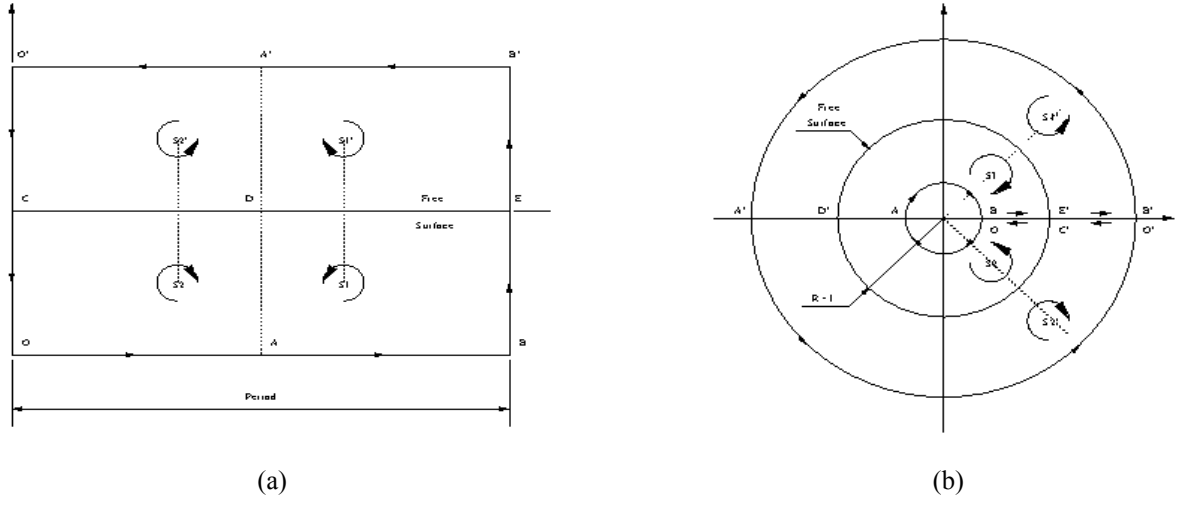


Figure 1. (a) A sketch of the z -plane with a set of two singularities and their images reflected onto the free surface. (b) The corresponding ζ -plane obtained via conformal mapping (11).

a pair of counter-rotating vortices and its corresponding image, the velocity potential ϕ_s can be expressed in the transformed plane by,

$$\phi_s(\zeta) = -k\mathcal{R} \left\{ i \log \left[\left(\frac{\zeta - \zeta_1}{\zeta - \zeta_2} \right) \left(\frac{1/\zeta - \bar{\zeta}_2}{1/\zeta - \bar{\zeta}_1} \right) \right] \right\}, \quad (12)$$

where k is the strength of the eddy couple in modulus. The first term inside the logarithm represents the contribution of the two vortices to the system, while the second term refers to their reflected images. The point vortices are prescribed to be at fixed positions in time. For a sink/source distribution and its corresponding image, the velocity potential ϕ_s takes the form,

$$\phi_s(\zeta) = k\mathcal{R} \left\{ \log \left[\left(\frac{\zeta - \zeta_1}{\zeta - \zeta_2} \right) \left(\frac{1/\zeta - \bar{\zeta}_1}{1/\zeta - \bar{\zeta}_2} \right) \right] \right\}. \quad (13)$$

Here k is defined as the volume flux per length unit of each of the sinks and sources. The contribution of the singularities to the “total” velocity \bar{u} is then given by $\nabla\phi_s$.

The singularities distributed beneath the free surface can induce varied surface current profiles, each of them with a certain minimum and maximum velocity and with a gentle or sharp current gradient. Figure (2) shows, respectively, the surface current profile induced by an eddy couple and by a distribution of 16 sinks and 16 sources, plus an arbitrary free surface initial condition. In this case the singularity distributions were conveniently chosen aiming to define “slowly” and “rapidly” varying surface currents.

3.4. Numerical scheme

Basically the method of solution consists of the following stages. Initially the full potential Φ is known on the surface for each time step. The potential ϕ_s due to the singularities is also defined and subtracted from the surface value of Φ such that the remaining surface wave potential ϕ_w , which has no singularities in the fluid domain, can be used with Cauchy's integral theorem to calculate the velocity $\nabla\phi_w$ on the free surface. Then the potential ϕ_s is added back in and corresponding “total” velocities are evaluated. The inclusion of the singularities necessitates the computation of the partial derivatives with respect to x and y of the velocity potential ϕ_s up to the third derivative, since the time-step criterion uses a Taylor series expansion truncated at the sixth power. Since in our model the singularities are assumed at fixed positions, the partial time derivatives vanish. Once an accurate converged solution is obtained for the full velocity potential Φ on the free surface, the cycle can begin again. Such stages are repeated until either the final time is reached, or the algorithm breaks down. Full details can be found in Dold (1992).

3.5. Accuracy

In the calculation of surface waves by the numerical scheme, it is important that a sufficient number of surface points is used in order to guarantee the accuracy of the numerical method. Waves described by only a few surface points

have their frequency and phase velocity underpredicted, with the percentage error decreasing rapidly the more points that describe each wavelength. However, an increase in the number of points used in the surface discretisation also leads to a significant increase in computing time and storage requirement. The surface discretisation points tend to drift

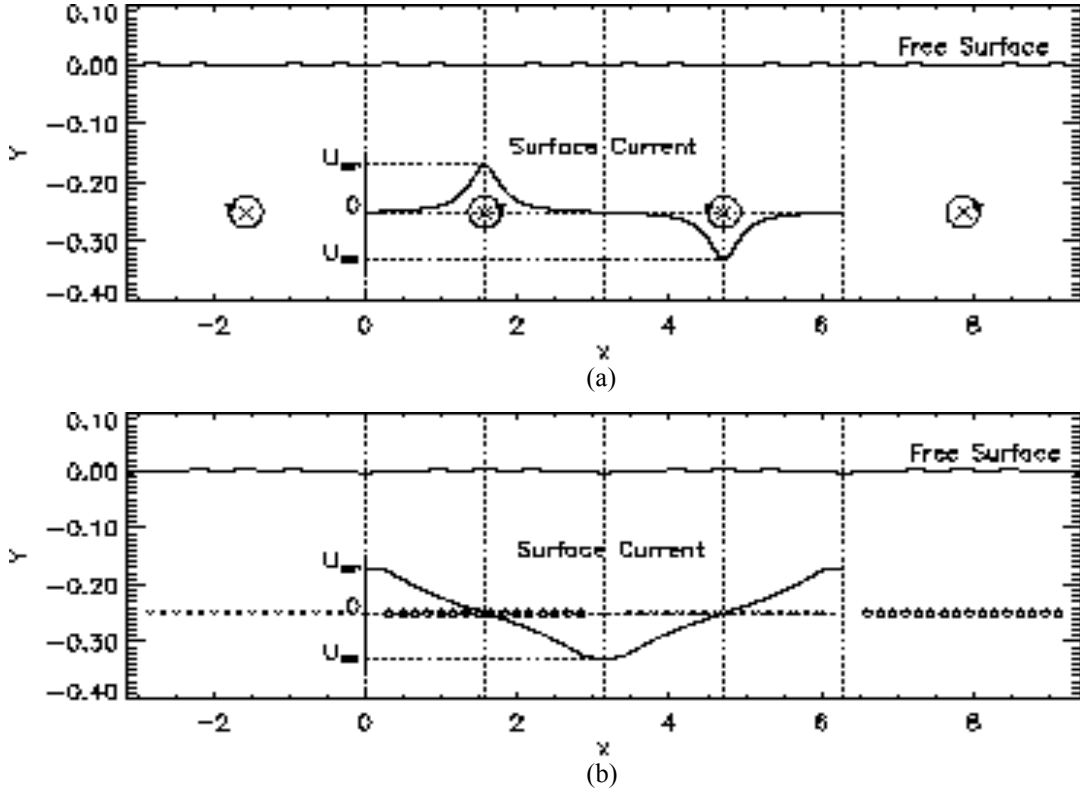


Figure 2. The surface current profile induced by: (a) an eddy couple: $U_{min}=-0.250 c_0$, $Fr=0.08$; (b) a sink-source distribution (x : sources, o : sinks): $U_{min}=-0.250 c_0$, $Fr=0.015$. In both cases 10 initial waves propagate from the left to the right side in deep water with $A_0 K_0=0.04$.

due to the surface current induced by the singularities, soon developing poor resolution of the surface waves. To ensure a smooth variation of surface variables with point number, a redistribution of points along the surface at regular intervals in time is done by using a tenth-order interpolation algorithm. The computed cases presented here have an initial distribution of 120 points per wavelength. To sum up no smoothing was introduced in the present computations in order to avoid any loss of information. The use of smoothing formulae based on the fitting of high order polynomials to the surface data was not required here since sawtooth numerical instabilities were well controlled by simply choosing an appropriate time step. Thus small waves with just two or three grid points and waves with sharp crests are not numerically dissipated by the scheme. All the computations presented in this work were done on a Sun Ultra 2/200.

4. Linear ray theory

Ray theory assumes that variations of wave amplitude A , frequency ω and wavenumber \mathbf{K} , together with current \mathbf{U} , are small over one wavelength. In other words any variations from uniformity are slow. Then the surface solution locally looks like a periodic plane wave train. For simplicity here we assume that the flow is in one dimension and that waves propagate in the direction of the current i.e. $\vec{K}=\vec{K}\hat{i}$. In the absence of surface tension effects and considering that the surface waves propagate in deep water, the surface wave dispersion relation is given by,

$$(\omega - UK)^2 = gK. \quad (14)$$

Note that ω is constant along a ray for a steady current. Assuming that initially the waves propagate in the positive direction with a phase velocity $c=(g/K)^{1/2}$ then,

$$\omega c^2 - gc - U = 0, \quad (15)$$

which is a quadratic determining the phase velocity c as a function of the surface current U and the frequency equation ω . Equation (15) gives two solutions for c ,

$$c = \frac{g}{2\omega} \left(1 \pm \sqrt{1 + \frac{4\omega U}{g}} \right) \quad (16)$$

The hypotheses assumed in the ray theory lead to equations which define lines parallel to the total group velocity C_g ($=dx/dt$), known as rays. In one dimension the ray equation in (x, t) simplifies to,

$$\frac{dx}{dt} = U(x) + c_g, \quad (17)$$

where c_g ($=c/2$) is the group velocity for waves in deep water relative to the water. Thus for a particular ray the quadratic (15) defines the frequency ω ,

$$\omega = g \left(\frac{1}{c_1} + \frac{U(x_0)}{c_1^2} \right) \quad (18)$$

where x_0 is the position of the ray at time $t=0$ and c_1 is the corresponding value of the phase velocity at that point. Substituting expression (18) into (16) gives,

$$c = \frac{1}{2} \frac{c_1^2}{U(x_0) + c_1} \left[1 \pm \sqrt{1 + 4U(x) \frac{U(x_0) + c_1}{c_1^2}} \right] \quad (19)$$

Restricting the initial conditions to the case with a positive sign (i.e. waves travelling in the same direction as the current), for time $t=0$, $x=x_0$, and then the ray equation (17) assumes the form,

$$\frac{dx}{dt} = U(x_0) + \frac{1}{2} c_1. \quad (20)$$

Expression (20) determines which root of c should be taken. If in the subsequent propagation of a ray $dx/dt=0$ then the wave is blocked by the current, followed by reflection with respect to the (x, t) plan. This corresponds to a transfer to the negative root of expression (16) for c . Thus energy cannot propagate beyond the blocking point and builds up along the caustic formed. Linear ray theory breaks down near the caustic and either nonlinear effects take over followed possibly by wave breaking, or a uniform solution is needed. The ray diagrams presented in the following section are obtained by integrating expression (20) with respect to x and t .

5. Ray diagrams and fully nonlinear results

5.1. "Slowly" varying surface currents

A sink/source distribution is employed to generate a near-linear surface current. 16 sinks and 16 sources are distributed symmetrically in the period domain at the same depth $d=0.25$. For a scheme of the fluid domain see figure (2b). The effect of the singularity distribution on the waves then depends on the strength k of the sinks and sources. For convenience we define k as the volume flux per length unit of each of the sinks and sources. The desired maximum and minimum velocities are then obtained choosing suitable values for k . The steady sinks and sources are "turned on" at time $t=0$ and impose a volume flux perpendicular to the plane of motion.

Figure (3) shows the evolution of short surface waves ($A_0 K_0=0.04$) interacting with a near-linear surface current ($U_{min}=-0.211 c_0$) plus their respective ray diagrams. The nonlinear results are vertically exaggerated 40 times. It is clear from figure (3a) the wave transformation that occurs due to the underlying current. Roughly speaking, a steep and a smooth region can be identified, respectively, downstream and upstream of the U_{min} region after a certain period of time. A strong increase in wave steepness is observed close to the U_{min} region, leading to wave breaking, while wave amplitudes decrease beyond this region. Some of the waves are steep enough to be noticeably affected by nonlinearity. It is possible to note that rays converge and overlap in figure (3b), with wave breaking taking place in the region where focusing occurs. Partial wave blocking is predicted by linear ray theory and thus confirmed by the nonlinear computations. When stronger currents are imposed, nonlinear effects take over before overlapping occurs; in this case a strong convergence of rays is observed nearby the U_{min} region. Figure (3b) also shows a low concentration of rays upstream of the U_{min} region, with waves much less steep in this place.

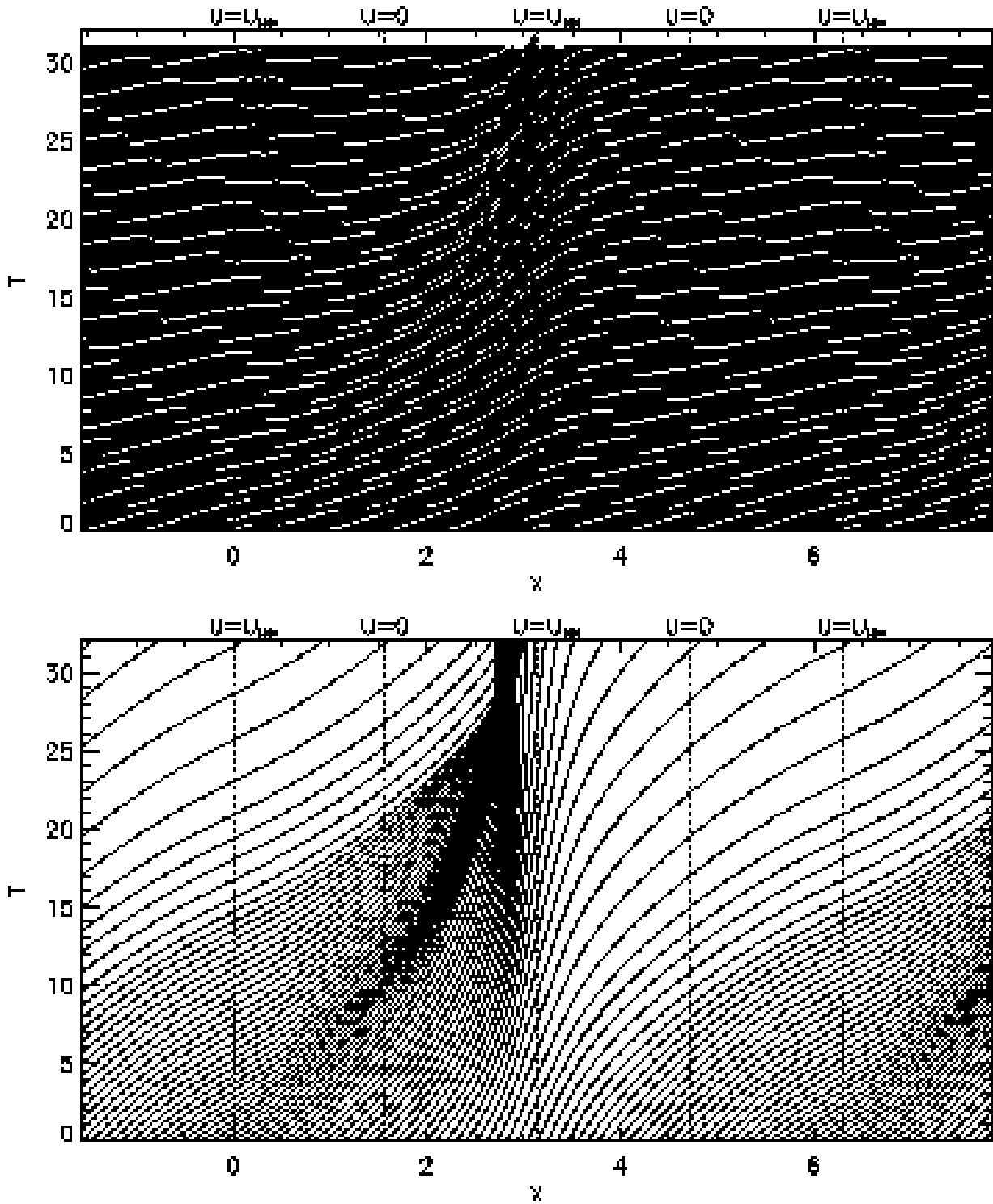


Figure 3. Fully nonlinear results (a) and its corresponding ray diagram (b) due to a near-linear current. $U_{min}=-0.211 c_0$, $K_0=10$, $A_0 K_0=0.04$. $t_{breaking}=31.0$. Vertical exaggeration 40:1.

Figure (4) shows the resolution of the breaking and reflected waves at time $t=31.0$. Breaking occurs isolated with the last remaining steep wave, with reflection being observed before wave breaking occurs, confirming that at least part of the wave energy that builds up within the caustic (see figure 3b) is released in the form of wave breaking and reflection. Partial reflection was also observed for computations with $U_{min}=-0.250 c_0$. Due to the steeper surface current gradient imposed, wave breaking occurs earlier in this case, with a less prominent wave reflection.

5.2. “Rapidly” varying surface currents

In this section “sharper” current gradients are imposed to the free surface when compared to the sink/source distribution. This is obtained by positioning a vortex couple underneath the free surface. For a scheme of the fluid domain see figure (2a). The maximum and minimum velocities are defined by choosing suitable values for the depth of

submergence d . Figure (5) shows in the same scale the stacked free surface deformation of a wave train and the corresponding ray diagram due to a stationary vortex dipole flow, with $U_{min} = -0.250 c_0$. This “rapidly” varying surface current is switched on at time $t=0$ and starts to interact with the wave train. The short waves have initial steepness of

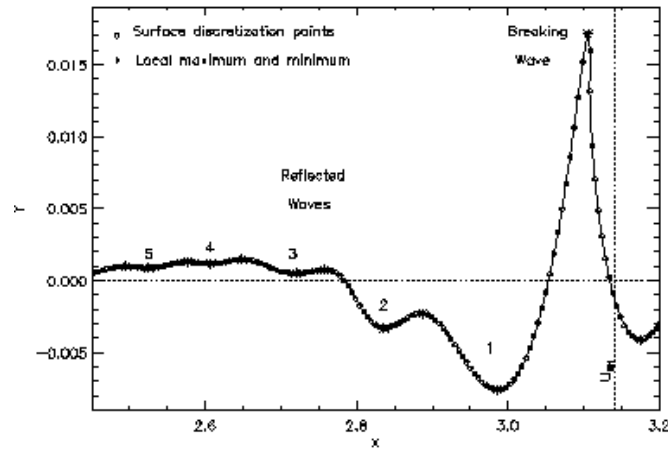


Figure 4. The corresponding reflected waves extracted from figure (3a) at breaking time ($t=31.0$).

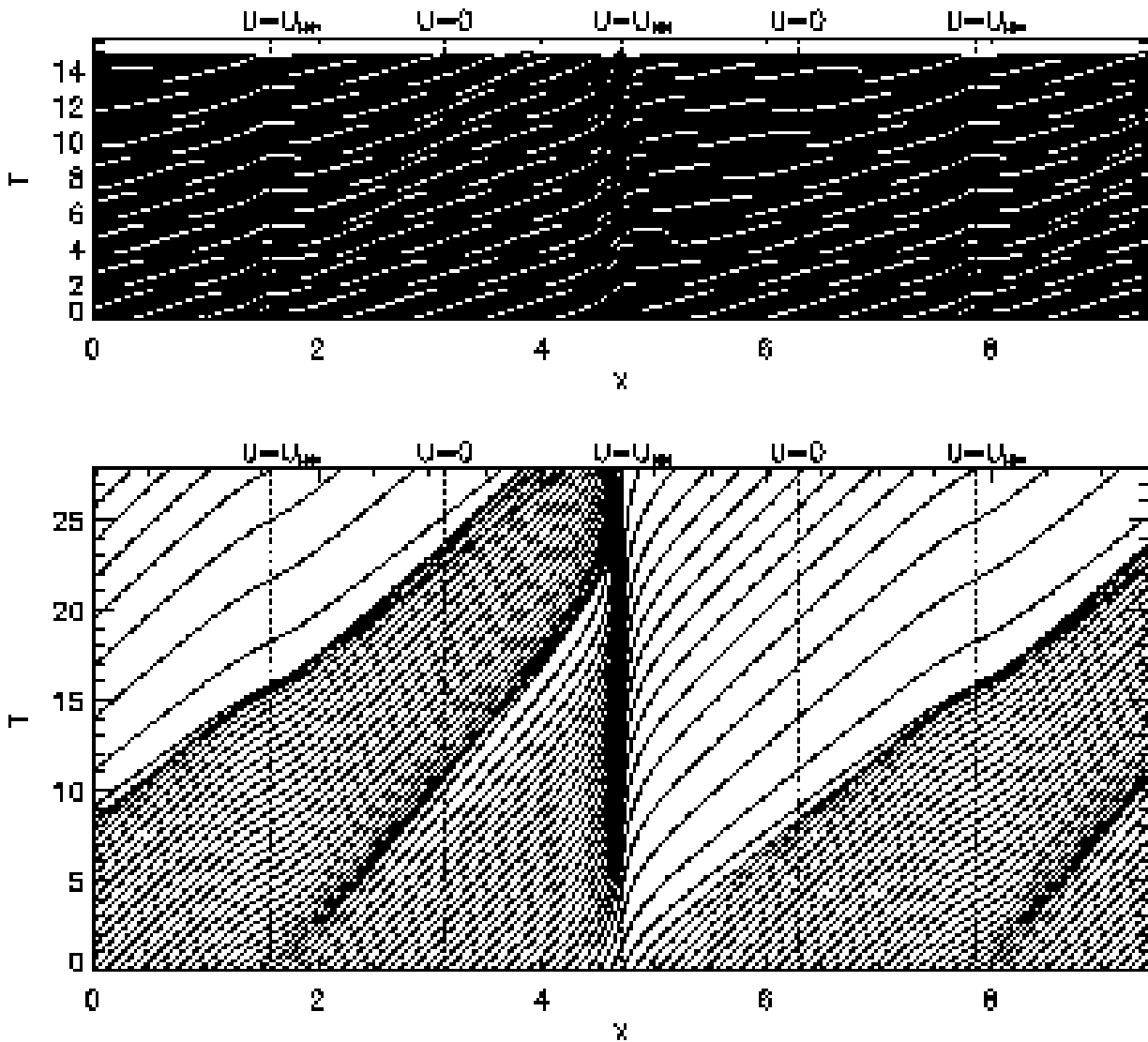


Figure 5. Fully nonlinear results (a) and its corresponding ray diagram (b) due to a “rapidly” varying surface current. $U_{min} = -0.250 c_0$, $K_0 = 10$, $A_0 K_0 = 0.04$. $t_{breaking} = 14.8$. Vertical exaggeration 40:1.

$A_0 K_0 = 0.04$. The fully nonlinear results show that surface currents induced by vortices are sufficient enough to cause wave steepening and breaking.

The wave transformation due to the underlying current is visible in figure (5a). The incident waves are clearly deformed near the maximum and minimum velocity regions U_{max} and U_{min} , while their group velocity remains unchanged near the regions where $U=0$. The positive current accelerates the surface waves nearby the U_{max} region, increasing locally their kinetic energy and group velocity, while in the U_{min} neighbourhood waves start to be partially blocked. These features are also confirmed by the ray diagram (5b), in which rays slow down when passing nearby the U_{max} region and become more rapid when near the U_{min} region.

A comparison with the ray diagram shows that rays strongly converge in the region where waves steepen and break. Though this region has a high concentration of rays, no focusing was observed. Since a strong surface current gradient is applied over one wavelength nearby the U_{min} region, ray theory assumptions are not fully satisfied there, with nonlinear effects taking over. Furthermore, since we are ignoring dissipation, in the light of the linear approximation wave action is conserved in the system as a whole. This implies that wave energy increases for rays moving into regions of greater frequencies and is lost when frequencies decrease. This feature is confirmed by the ray diagram (5b), where rays are clearly more spaced upstream of the U_{min} region than downstream.

Wave properties measured from the nonlinear calculations at breaking time $t=14.8$ and from linear ray theory are provided in figure (6). The linear results are evaluated based on the value of the frequency ω of the appropriate ray. From the ray diagram (5b) it is possible to see that this corresponds to a ray initially located in the region where the surface current vanishes. Figure (6d) shows the discretisation of the breaking wave for the required accuracy provided. The breaking wave takes the form of a breaker jet, with the points near the tip tending to move together. Its amplitude is approximately 4 times A_0 , the initial wave amplitude (see figure 6b). Breaking wave tests carried out by Chawla (1999) also observed that amplitude dispersion plays an important role in determining wave blocking due to the rapid increase in wave steepness close to the blocking point. Because of these substantial amplifications, waves become too steep to be described by an infinitesimal wave theory.

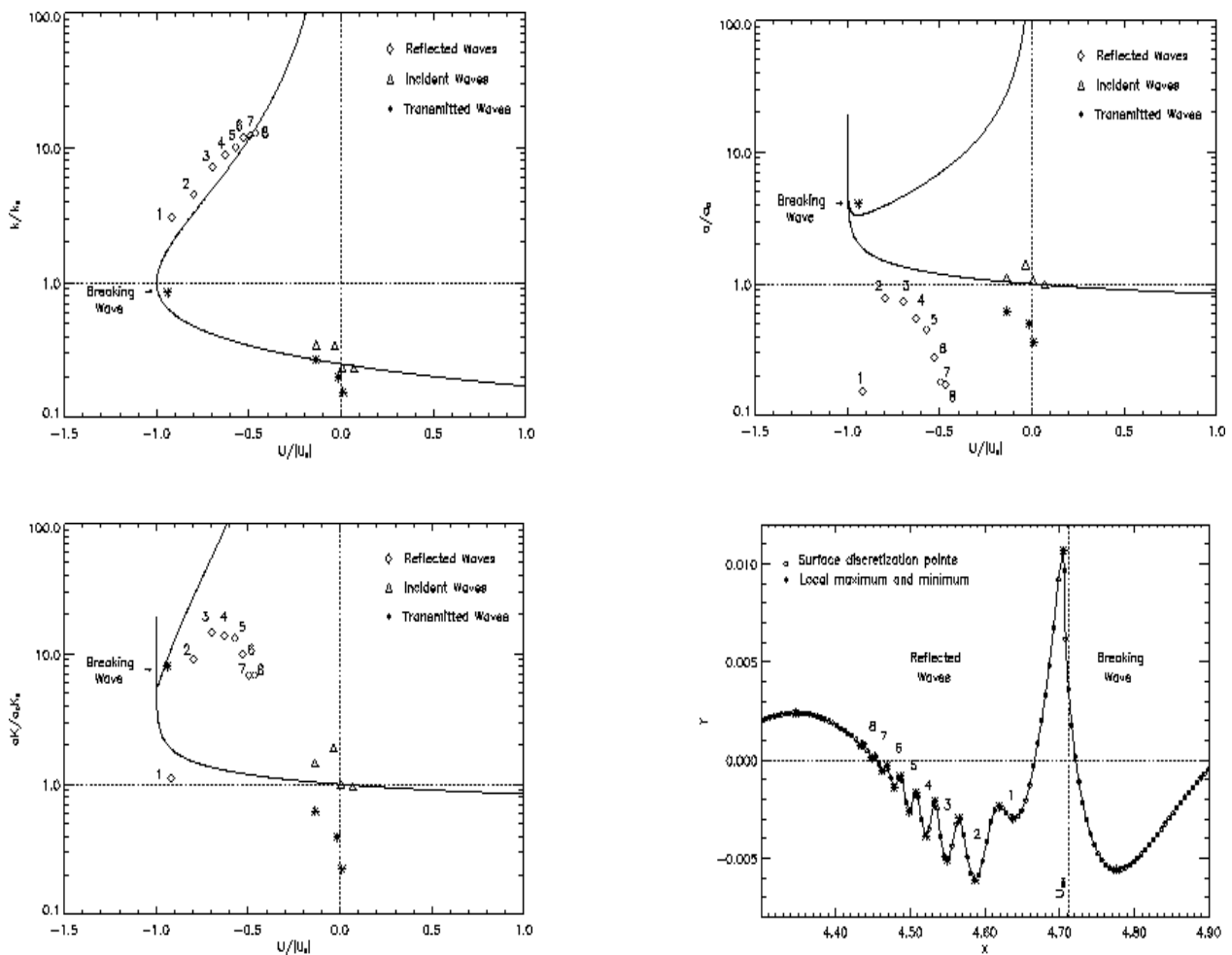


Figure 6. Variation of wavenumber (a), amplitude (b), and wave steepness (c), according to linear ray theory (-----) and obtained from the fully nonlinear results; the reflected waves (d) extracted from figure (5a) at breaking time ($t=14.8$).

Figure (6d) also shows the discretisation of the reflected waves formed behind the breaking wave. Waves 2 and 3 are particularly well resolved with a minimum of 6 points per wavelength, which represents a reasonable discretisation for gentle waves (for details see Dold 1992). Indeed a comparison between the wavenumbers reveals a good agreement between linear and nonlinear results (see figure 6a). A closer look at figures (6b) and (6c) shows that wave steepnesses tend to agree better against ray theory than wave amplitude results. This agreement becomes even better for initially more gentle wave steepnesses. From figure (6c) it is possible to verify that incident waves have their steepness increased when on adverse currents, leading to wave breaking close to the minimum velocity U_{min} , while transmitted waves decrease their steepness substantially, becoming smoother for positive currents.

6. Summary

We have attempted to simulate the interaction between water waves and currents with special attention to the effects of nonlinearity on the free surface. This was motivated by several theoretical and recent experimental works on the matter. A fully nonlinear model was developed in order to understand the interaction of stationary submerged currents induced by singularities with a large number of short surface waves. The nonlinear numerical results show that adverse currents induce wave steepening and breaking. Furthermore the wave transformation induced by the underlying currents can be identified by a steep and a smooth region formed, respectively, downstream and upstream the U_{min} region after a certain period of time. A strong increase in wave steepness is observed within the blocking region, leading to wave breaking, while wave amplitudes decrease significantly beyond this region.

The nonlinear results obtained for “slowly” varying currents agree well with linear ray theory. In fact in this case ray theory results are complemented by the accurate fully nonlinear computations. For very small initial wave steepnesses these computations give accurate linear solutions. The numerical simulations also show that wave blocking and breaking are more prominent for sharp surface current gradients. For these cases the nonlinear results reveal that reflection does occur nearby the U_{min} region for sufficiently strong adverse currents, thus confirming that at least some of the wave energy that builds up within the blocking region can be released in the form of partial reflection, which applies to very gentle waves, and wave breaking, even for small amplitude waves.

7. Acknowledgement

I am grateful for the guidance and useful discussions with Prof. D.H.Peregrine of the School of Mathematics, University of Bristol. I acknowledge the financial support through CAPES, the brazilian agency for post-graduate education, and Fluminense Federal University.

8. References

- Chawla, A., 1999, “An Experimental Study on the Dynamics of Wave Blocking and Breaking on Opposing Currents.” PhD thesis, University of Delaware, U.S.A.
- Chawla, A. & Kirby, J.T., 2002, “Propagation of weakly non-linear, narrow-banded waves against strong currents.” Submitted for publication.
- Dold, J.W., 1992, “An Efficient Surface-Integral Algorithm Applied to Unsteady Gravity Waves.” *J. Comp. Phys.*, v. 103, pp. 90-115.
- Dold, J.W. & Peregrine, D.H., 1986, “An Efficient Boundary-Integral Method for Steep Unsteady Water Waves.” In *Numer. Meth. for Fluid Dynamics II*, Eds. K.W. Morton & M.J. Baines, pp. 671-679.
- Jonsson, I.G., 1990, “Wave-current interactions.” In *The Sea, Ocean Engng. Science 9A*, Eds. B. Le Mehaute & D.M. Hanes, pp. 65-120.
- Moreira, R.M., 2001, “Nonlinear interactions between water waves, free surface flows and singularities.” PhD thesis, University of Bristol, U.K.
- Moreira, R.M. & Peregrine, D.H., 2001, “Interactions between water waves and singularities.” In *IUTAM Symp. on Free Surface Flows*, Eds. A.C. King & Y.D. Shikhmurzaev, pp. 205-212.
- Peregrine, D.H., 1976, “Interaction of water waves and currents.” *Adv. Appl. Mech.* 16, pp. 9-117.
- Peregrine, D.H. & Smith, R., 1979, “Nonlinear effects upon waves near caustics.” *Phil. Trans. R. Soc. Lond.* A292, pp. 341-370.
- Peregrine, D.H. & Thomas, G.P., 1979, “Finite-amplitude deep-water waves on currents.” *Phil. Trans. R. Soc. Lond.* A292, pp. 371-390.
- Suastika, I.K., de Jong, M.P.C. & Battjes, J.A., 2000, “Experimental study of wave blocking.” *Proc. 27th Internat. Conf. on Coastal Engng.*, Sydney, ASCE, pp. 223-240.
- Thomas, G.P. & Klopman, G., 1997, “Wave-current interactions in the nearshore region.” In *Gravity Waves in Water of Finite Depth*, Ed. J.N. Hunt, pp. 215-319.

9. Copyright notice

The author is the only responsible for the printed material included in this paper.